On Facts and Artefacts: The Difficulty to Evaluate an Artificial Nuclease

by **Stefan Pitsch**[a]), **Ute Scheffer**[b]), **Markus Hey**[b]), **Andreas Strick**[b]), and **Michael W. Göbel***[b])

[a]) Institut de Chimie Moléculaire et Biologique, Ecole Polytechnique Fédérale de Lausanne (EPFL), BCH-LCAN, CH-1015 Lausanne (fax: +41216939355; e-mail: stefan.pitsch@epfl.ch)

[b]) Institut für Organische Chemie und Chemische Biologie, Johann Wolfgang Goethe-Universität Frankfurt, Marie-Curie-Str. 11, D-60439 Frankfurt am Main (fax: +496979829464; e-mail: M.Goebel@chemie.uni-frankfurt.de)

Dedicated to Professor *Duilio Arigoni* on the occasion of his 75th birthday

A number of promising synthetic catalysts for the hydrolytic degradation of RNA have been developed in recent years. Some of them show remarkable selectivity for pyrimidine nucleotides. The general problem of all these studies is to distinguish between real effects and artefacts caused by traces of contaminating natural ribonucleases. We show that methods representing the current state of the art (diethylpyrocarbonate treatment, sterilization, ultrafiltration, *etc.*) do not sufficiently protect against severe artefacts. However, an incorruptible assay could be found by comparing the cleavage of RNA and its mirror image. Enantiomeric RNA is completely resistant to enzymatic degradation, whereas achiral nonpeptide catalysts, by fundamental laws of symmetry, cannot distinguish between enantiomers and will induce exactly the same cleavage pattern with both substrates.

Introduction. – Catalysts that induce the hydrolytic degradation of RNA are an important issue of chemical research. Such artificial ribonucleases are mostly based on metal complexes [1], however, some metal-free systems are known as well [2–4]. They generally consist of oligo amines [4], guanidines, or structurally analogous heterocycles [2][3]. In recent years, we have studied the catalysis of phosphoryl-transfer reactions by guanidinium salts {3-[(guanidino)methyl]phenyl}methylguanidine (**1b**) and 2-[(3-{[(4,5-dihydro-1*H*-imidazol-2-yl)amino]methyl}phenyl)methyl]amino-4,5-dihydro-1*H*-imidazole (**2b**) [5][6]. With highly reactive model substrates in dipolar aprotic solvents, large rate increases could be observed. In aqueous solution and with RNA substrates, however, the catalytic efficiency decreased to low values. In an attempt to optimize compounds **1b** and **2b** for RNA cleavage, a series of guanidine mimics have been synthesized recently [7]. The most striking effects in this series were observed with 2-[(3-{[(1*H*-benzimidazol-2-yl)amino]methyl}phenyl)methyl]amino-1*H*-benzimidazole (**3b**), a close structural analogue of **1b** and **2b**. The increase of catalytic potential has been attributed to a change in pK_a from $\sim$14 to 7. A further jump in reactivity was seen with the HCl salt of *N*-(1*H*-benzimidazol-2-yl)-*N*′,*N*′-bis[2-(1*H*-benzimidazol-2-ylamino)ethyl]ethane-1,2-diamine (**4b**), which is equipped with three aminobenzimidazole units. Both compounds **3b** and **4b** led to well-reproducible cleavage data and did not show a significant preference for certain nucleotides. In contrast, other candidates investigated during recent years, for example, the HCl salt of *N*-(4,5-dihydro-1*H*-imidazol-2-yl)-*N*′,*N*′-bis[(4,5-dihydro-1*H*-imidazol-2-ylamino)ethyl]ethane-1,2-diamine (**5b**), occasionally showed irregular concentration-effect correlations. These observations and the pronounced selectivity for pyrimidines typical for those compounds led to

the suspicion that contamination with natural ribonucleases might be the true source of RNA cleavage activity (the majority of ribonucleases seem to be specific for pyrimidines [8]). We will present below experiments designed to distinguish between effects of true catalyst-induced RNA cleavage and those of protein contaminants. This has proven to be no trivial task. A definitive answer finally was derived from cleavage experiments with enantiomeric-RNA oligonucleotides [9][10], which are completely resistant to chiral enzyme catalysts [9]. Achiral catalysts, however, are expected to produce identical cleavage patterns with both substrate enantiomers.

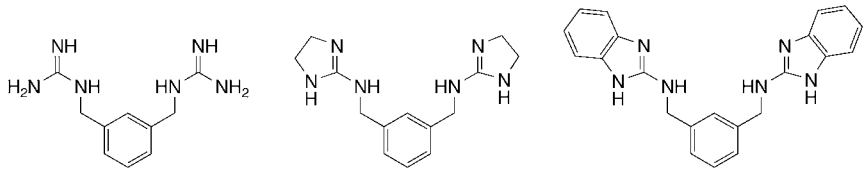

1 **2** **3**

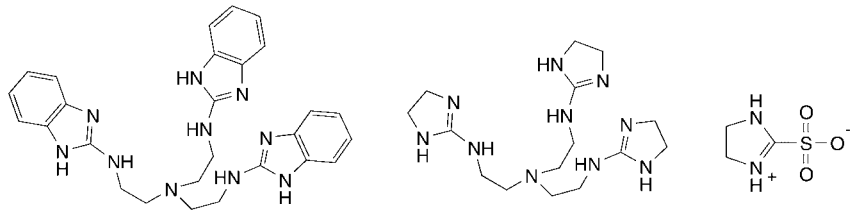

4 **5** **6**

Results. – Trisguanidinium picrate **5a** was prepared in one step from tris-(2-aminoethyl)amine and the 4,5-dihydroimidazole-2-sulfonic acid (**6**; 26%) [11]. Similar oligoguanidines had been reported before as anion receptors by *Lehn* and co-workers [12]. Ion exchange easily led to the water-soluble hydrochloride **5b**.

RNA Hydrolysis induced by **5b** was studied initially with the dye labeled substrate **7**. The fluorescent cyanine dye allows detection of the RNA and of all degradation products with high sensitivity on a DNA sequencer [7][13–15]. A short stretch of DNA (T_{10}) was placed between the dye and the RNA sequence to prevent the formation of very short fragments that would complicate the electrophoretic separation (the RNA part of oligonucleotides **7** and **8** is adopted from [16]). RNA Hydrolysis is normally initiated by nucleophilic attack of 2′-OH at the P-atom [3]; DNA, lacking the 2′-OH group, is known to be stable under the conditions of RNA cleavage. In an improved version of the substrate, a T_4 fragment was attached to the 3′-end (**8**). *Fig. 1* gives a survey of the oligonucleotides used in this study. A second type of RNA substrate (**13**–**15**), constructed in a similar way, contained a stem-loop element from HIV-1 TAR [17].

When incubated with a 10 mM solution of the salt **5b** (pH 7, 37°, 16 h), substrate **7** was hydrolyzed to a considerable degree. In *Fig. 2*, *lane b*, an example showing 54% conversion of **7** is given. However, most other experiments ended with more than 95% substrate degradation. At 1 mM **5b**, typically 35% of the substrate was hydrolyzed and,

7 Cy5-T_{10}-ribo(CUAGCCGACUGCCGAUCUCGCUGACUGAC)$^{3'}$

8 Cy5-T_{10}-ribo(CUAGCCGACUGCCGAUCUCGCUGACUGAC)-$T_4^{3'}$

9 Cy5-dC_{15}-T_3-ribo(U-3',5')-$T_2^{3'}$

10 Cy5-dC_{21}-T_3-ribo(U-2',5')-$T_2^{3'}$

11 Cy5-dC_{11}-ribo(U-3',5'-U-3',5'-U-3',5'-U-3',5'-U-3',5'-U-3',5')-$dC_4^{3'}$

12 Cy5-dC_{24}-ribo(U-2',5'-U-2',5'-U-2',5'-U-2',5'-U-2',5'-U-2',5')-$dC_4^{3'}$

13 Cy5-T_{20}-ribo(GGCCAGAUCUGAGCCUGGGAGCUCUCUGGCC)$^{3'}$

14 Cy5-T_{10}-ribo(GGCCAGAUCUGAGCCUGGGAGCUCUCUGGCC)-$T_4^{3'}$

15 Cy5-linker-T_{10}-*ent*-ribo(GGCCAGAUCUGAGCCUGGGAGCUCUCUGGCC)-$T_4^{3'}$

16 TGTGGAATTGTGAGCGGATA$^{3'}$

17 Cy5-T_{20}-riboU$^{3'}$

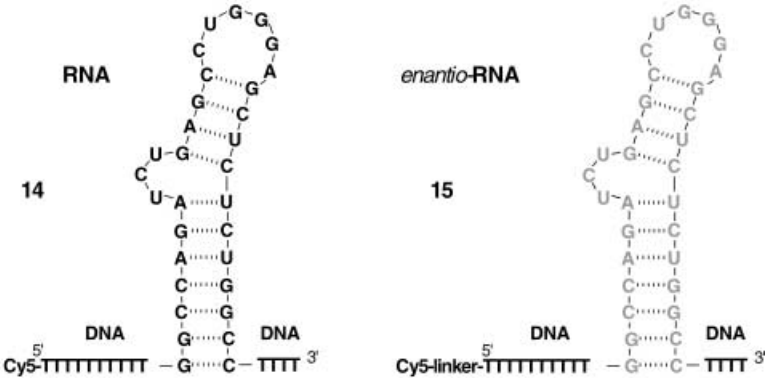

Fig. 1. Top: *Oligonucleotides used in this study.* Bottom: *Secondary-structure model of the TAR-derived sequences* **14** *and* **15**. Enantiomeric nucleotides are symbolized by grey letters.

at 0.1 mM, 3.4%. By coincidence of peaks with a ladder of all possible hydrolytic fragments, cleavage sites could be localized [7][13][14]. All fragmentations occurred after pyrimidine nucleotides. Since the conformational requirements for an in-line attack of 2′-OH are not given in regular duplex structures, cleavage normally occurs at sites of increased flexibility such as bulges or loops. The observed pattern fits with the secondary-structure model depicted in *Fig. 1*[1]). Thus, compound **5b** in contrast to the benzimidazole **4b** [7], does not denature RNA secondary structures.

---

[1]) An interesting, yet unexplained observation is cleavage after C(19), a nucleotide expected to participate in the lower stem region of TAR (see also [6][7]).

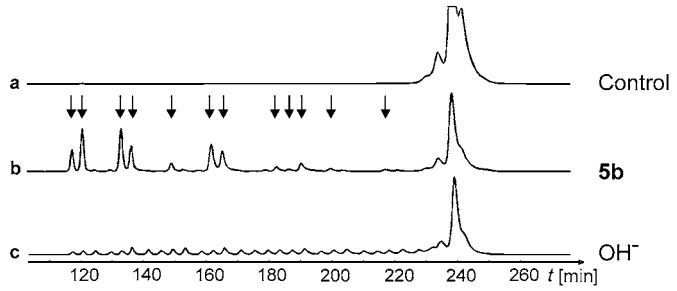

Fig. 2. *Cleavage of substrate* **7** *induced by compound* **5b**. Control: Incubation of **7** in buffer for 16 h at 37° (*lane a*). RNA Cleavage shown in *lane b* was performed at 10 mM catalyst concentration in 50 mM *Tris*-HCl, 0.01% SDS buffer (pH 7.0). A base ladder of substrate **7** is depicted in *lane c*. RNA fragmentation was analyzed as described in the *Exper. Part*. Cleavage sites indicated by arrows are given in bold letters: Cy5-T_{10}-**C**UAG**CC**GA**C**UG**CC**GAU**CUC**G**C**UGA**C**UGAC.

Well aware of the danger of RNase contamination, a wide range of precautions had been taken. Reaction vessels, buffers, and all robust constituents were treated with diethylpyrocarbonate (DEPC) prior to sterilization. Solutions of **5b** and other catalyst candidates were purified by ultrafiltration. This technique should remove globular molecules larger than 3 kDa [7][18][19]. As a test, RNase A (1 ng/ml) was added to RNA substrate **7** to produce a highly contaminated sample. Very short incubation times were sufficient for complete degradation of **7** (*Fig. 3*, *lane c*). The same RNase A solution was then subjected to ultrafiltration. When RNA **7** was mixed with the filtrate, no cleavage occurred even after long incubation times (*lane b*). Purification of a solution of trisguanidine **5b** by this method followed by incubation with RNA **7**, led to cleavage patterns indistinguishable from those shown in *Fig. 2*. It seemed rather safe to conclude, at this point, that trisguanidine **5b** itself is capable of catalysis of RNA degradation.

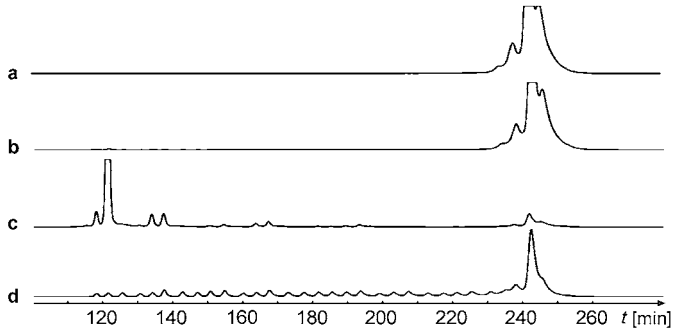

Fig. 3. *Ultrafiltration to remove RNase contaminants. Lane a:* Substrate **7** incubated for 20 h at 37°. *Lane c:* Substrate **7** after incubation with RNAse A (1 ng/ml enzyme, 5 min, 37°). *Lane b:* The same solution of RNAse A was subjected to ultrafiltration and incubated with **7** for 20 h at 37°. A base ladder of **7** is shown in *lane d*.

In the next set of experiments, the influence of several additives was investigated (*Fig. 4*). High concentrations of NaCl are expected to prevent ion-pair association of trisguanidinium cations and RNA. As foreseen, 1M NaCl completely abolished cleavage

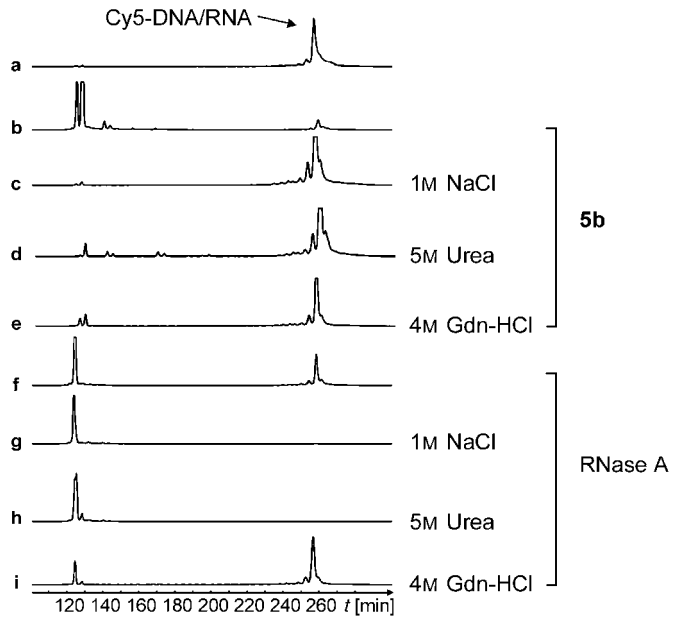

Fig. 4. *RNA Cleavage by compound* **5b** *and RNase A in the presence of different salts* (50 mM *Tris*-HCl/0.01% SDS buffer, pH 7.0, 24 h, 37°). *Lane a:* Untreated substrate **8** as a negative control. Substrate **8** was incubated with catalyst **5b** (4 mM) in the absence (*lane b*) or presence of 1M NaCl (*lane c*), 5M urea (*lane d*), or 4M guanidinium hydrochloride (Gdn-HCl, *lane e*). The same set of experiments was repeated with 10 ng RNase A: 1M NaCl (*lane g*), 5M urea (*lane h*), 4M Gdn-HCl (*lane i*).

induced by **5b**, whereas RNase A was not inhibited. Addition of 5M urea led to comparable results. As a classical reagent for denaturing proteins, 4M guanidinium chloride blocked RNase A. That catalysis by **5b** was inhibited as well may be explained by ion-pair disruption. While denaturation of a contaminating RNase cannot be ruled out, these data still favor the interpretation that **5b** is the active catalyst. This view was challenged for the first time when RNase inhibitors were found to suppress strand degradation (*Fig. 5*).

The experiment designed to unravel the conflicting data was to compare cleavage of the oligonucleotides **9** and **10**. Substrate **9** contains a single 3′,5′-linked ribonucleotide in a stretch of DNA, while, in compound **10**, the ribonucleotide has a 2′,5′ linkage. Furthermore, the total length of the DNA spacer of **10** is extended relative to **9**, allowing simultaneous monitoring of both substrates in a single analysis (*Fig. 6*,*a*, *lane a*). As shown in *lane c*, both substrates are sensitive to base-induced hydrolysis. In contrast, RNase A attacks only the natural 3′,5′ bond: the small amount of cleavage seen with substrate **10** did not increase with time (*Fig. 6*,*b*, *lanes a* and *b*) or with increasing amounts of RNase A (data not shown). We explain this as cleavage of contaminating isomeric 3′,5′ strands present in **10**. It is known that 2′- or 3′-silylated ribonucleosides may isomerize to a small extent during the process of phosphoramidite formation [20]. Unfortunately, the amount of cleavage induced by **5b** was too small even after 20 h to decide whether substrate selectivity exists or not (*Fig. 6*,*a*, *lane b*).

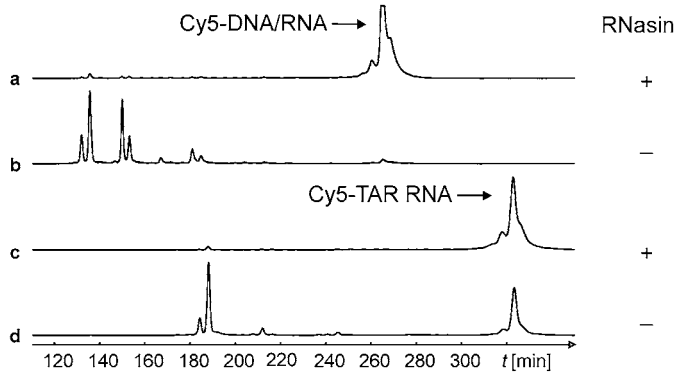

Fig. 5. *Influence of RNase inhibitor.* Substrates **7** and **13** were incubated with trisguanidine **5b** (10 mM) in presence (*lanes a* and *c*) or absence (*lanes b* and *d*) of 1 unit/μl RNase inhibitor. Samples were run in parallel on denaturing PAGE.

In a similar way, we constructed the substrate pair **11** and **12**, the first containing six 3′,5′-linked uridines, the second the corresponding 2′,5′-hexa-uridine sequence (*Fig. 6,a*, *lane d*). Upon base-induced cleavage, the 2′,5′-linked substrate was distinctly more reactive (*lane f*). However, in the presence of **5b**, selective cleavage of the 3′,5′-linked substrate **11** occurred. 3′,5′-Selective hydrolysis is also induced by RNase A (*Fig. 6,b*, *lanes c* and *d*). Here, again, the digestion of the 2′,5′-substrate stopped at low levels, irrespective of enzyme concentration and reaction time (data not shown). A positively charged anion receptor such as **5b** may catalyze RNA hydrolysis by electrostatic transition-state stabilization [2][3][7], and, while it is reasonable not to expect high levels of 3′,5′ selectivity from this mechanism, it cannot be excluded in a strictly logical sense. The experiments shown in *Fig. 6*, therefore, give strong evidence for, but not proof of, contamination effects.

At this stage, two groups of assays convincingly advocated contradicting explanations. To corroborate the suspicion of artefacts, an incorruptible test was needed. The assay designed to meet this requirement makes use of enantiomeric RNA substrates. Since **5b** is an achiral molecule, it forms enantiomorphous complexes with RNA and its mirror image. The transition states of catalysis are also expected to be enantiomorphous, leading to indistinguishable cleavage patterns for the enantiomeric RNA substrates. The RNA part of substrate **15** is the exact mirror image of the RNA parts of compounds **13** and **14**. Enantiomeric nucleoside building blocks were prepared from D-glucose according to published procedures [10] and assembled as 2′-*O*-tom-protected phosphoramidites [21]. The *enantio*-RNA is embedded into DNA (natural configuration) and has a fluorescent dye attached to the 5′ end *via* conventional amino linker/active ester chemistry. After isolation by HPLC, **15** still contained traces of shorter fragments that were absent in the PAGE-purified sample of **14** (*Fig. 7,a*, *lanes a* and *d*). Base-induced hydrolysis of **14** and **15**, as expected, led to identical cleavage patterns (*lanes c* and *f*). In contrast, when **5b** was added, RNA hydrolysis was found to be enantioselective (*lanes b* and *e*) and, as seen with **7** (see *Fig. 2*), pyrimidine specific. These findings clearly demonstrate that the active catalyst in the sample of **5b** must be a chiral molecule, *e.g.*, a ribonuclease or another protein, but not **5b** itself. Controls with

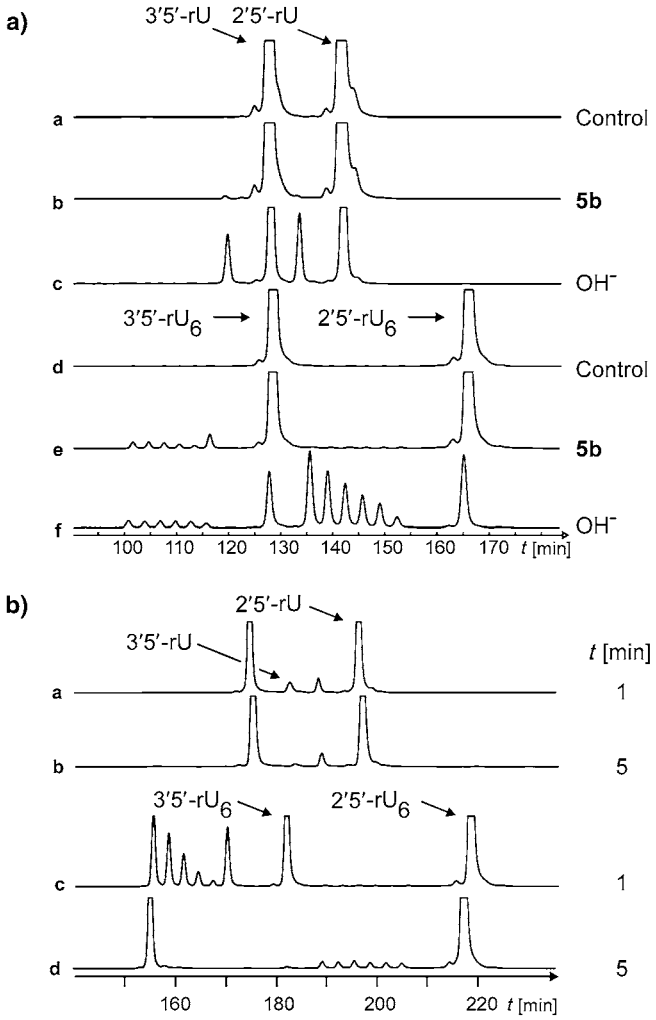

Fig. 6. a) *Cleavage of the 3′,5′-linked substrates* **9** (3′,5′-rU), **11** (3′,5′-rU$_6$), *and their 2′,5′-linked counterparts* **10** (2′,5′-rU) *and* **12** (2′,5′-rU$_6$) *by* **5b** (*cf. Fig. 1*). Different spacer lengths allow analysis of the reaction of both substrate types in the same experiment; **5b** (10 mM) was incubated for 20 h at 37° with either a mixture of **9** and **10** (*lane b*) or **11** and **12** (*lane e*) in 50 mM *Tris*-HCl/0.01% SDS buffer (pH 7.0). Untreated controls are shown in *lanes a* (**9** and **10**) and *d* (**11** and **12**), base ladders are depicted in *lane c* (**9** and **10**) and *f* (**11** and **12**). b) *RNase A Treatment of substrates* **9**–**12**. Oligonucleotides were incubated with 1 ng/ml RNase A for 1 min (**9** and **10**: *lane a*; **11** and **12**: *lane c*) or 5 min (**9** and **10**: *lane b*; **11** and **12**: *lane d*) at 37°. Samples were run in parallel on denaturing PAGE.

RNase A and RNase T1 are shown in *Fig. 7,b*. Both enzymes are specific for the natural stereoisomer of RNA. *Fig. 7,c* shows RNA cleavage induced by the catalyst **4b**. The patterns of both stereoisomers are indistinguishable. It can be safely concluded, therefore, that the active catalyst is compound **4b** itself and not a protein contaminant.

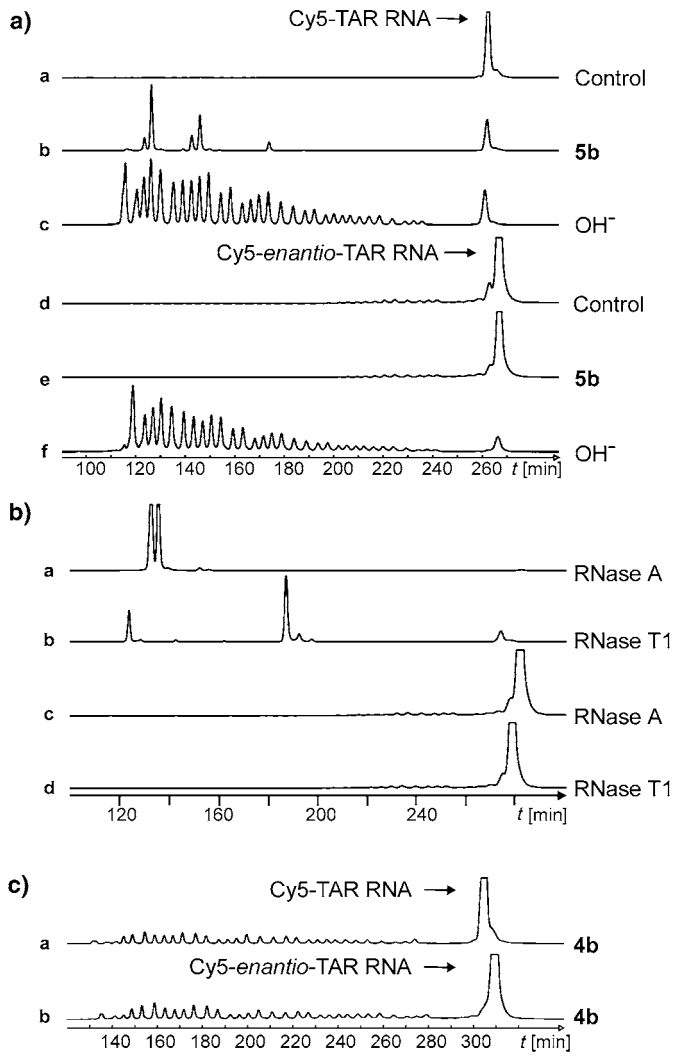

Fig. 7. *Cy5-TAR RNA and Cy5*-enantio-*TAR RNA*. *a*) The cleavage pattern produced by **5b** (10 mM) with RNA **14** (*lane b*) is compared to that with *enantio*-RNA **15** (*lane e*). Controls contain only Cy5-labeled RNA substrates (**14**: *lane a*; **15**: *lane d*). Base ladders are shown in *lane c* (**14**) and in *lane f* (**15**). *b*) Cy5-labeled TAR (*lanes a* and *b*) and *enantio*-TAR RNA (*lanes c* and *d*) were incubated with 10 ng RNase A and 1 unit RNase T1, respectively. *c*) Nonspecific base-cleavage pattern produced by **4b** with TAR RNA **14** or *enantio*-TAR RNA **15**. Samples were run in parallel on denaturing PAGE.

Discussion. – At first glance, the characterization of an artificial ribonuclease seems not to be a challenging task; many examples have been described and major problems have rarely been reported. However, as shown above, the risk of producing artefacts is high. While proper laboratory techniques and ultrafiltration help to minimize protein-related artefacts, contamination may not be strictly ruled out. Interpretation of

experiments performed with low concentrations of long RNA's incubated over many hours is treacherous. When selectivity for pyrimidines is observed, as is common in the literature, contamination should be suspected. Enantiomeric RNA is a powerful tool in these cases to separate true catalysis from artefacts when achiral catalysts are used. Studies with chiral catalysts ideally should compare the enantiomorphous systems catalyst/RNA and *ent*-catalyst/*ent*-RNA leading to identical cleavage patterns. Unfortunately, enantiomeric RNA is a precious material not routinely accessible to every researcher. As an alternative, experiments with RNase inhibitors may be considered, although variable degrees of inhibition render data interpretation less straightforward.

A disquieting question remains to be answered. What is the agent responsible for RNA degradation in the presence of trisguanidine **5b**, and what is its source? RNA Samples showed no trace of hydrolysis without **5b**. Buffer and substrate, therefore, seem to be free of ribonucleases. The amount of cleavage observed correlates with the concentration of 'catalyst'. Ultrafiltration, on the other hand, should remove proteins from solutions of **5b**. A possible hint comes from experiments with the benzimidazole catalyst **4b**. When RNA degradation was measured as a function of catalyst concentration, a sudden loss of activity was found within a narrow concentration range around 100 μM [7]. Above the borderline, formation of large aggregates of **4b** and the stable RNA model **17** could be observed by fluorescence correlation spectroscopy (FCS) [7][22]. The diffusion time of **17** calculated from the autocorrelation function was 160 μs in pure buffer (*Fig. 8,a*). The data could be nicely fitted to a one-component model (*Fig. 8,b* and *c*). Upon addition of **4b**, this value increased dramatically (*Fig. 8,d*).

Because of the heterogeneous nature of the aggregates, a fit of experimental and calculated data was no longer possible (*Fig. 8,e* and *f*). Aggregation is accompanied by denaturation of RNA secondary structure. At the borderline, however, the non-selective-cleavage pattern changes to a pyrimidine-selective pattern, reflecting the stem-bulge-loop secondary structure of **13** (*Fig. 9,b*). At slightly reduced concentrations of **4b**, all cleavage effects disappear. When repeated with enantiomeric RNA **15** (not shown), the same correlation of catalyst concentration and cleavage was observed, however, with one exception. Pyrimidine selective hydrolysis did not occur at any stage. A possible explanation is based on the assumption that minor traces of ribonuclease – invisible in the controls – might be captured and enriched to significant local concentration by the aggregates of RNA and compound **4b**. At high concentrations, ribonucleases might be either denatured by the aggregates or their activity is surpassed by the efficient catalyst **4b**. At low concentration, aggregates disappear, thus abolishing colocalization of ribonucleases and their substrates. However, when the interaction of **5b** and oligonucleotide **17** (or a mixture of **16** and **17**) was studied by FCS, no aggregates were observed up to 10 mM of **5b** (not shown). A second tentative explanation is based on the assumption that covering a strand of RNA with guanidinium salts such as **4b** and **5b** promotes in some way the complexation with ribonucleases. What both working hypotheses have in common is the idea of induced colocalization of ribonucleases and nucleic acids. This phenomenon should be detectable by FCS. The objectives of our present work are to investigate the mechanism of benzimidazole catalyzed RNA hydrolysis, to synthesize conjugates of

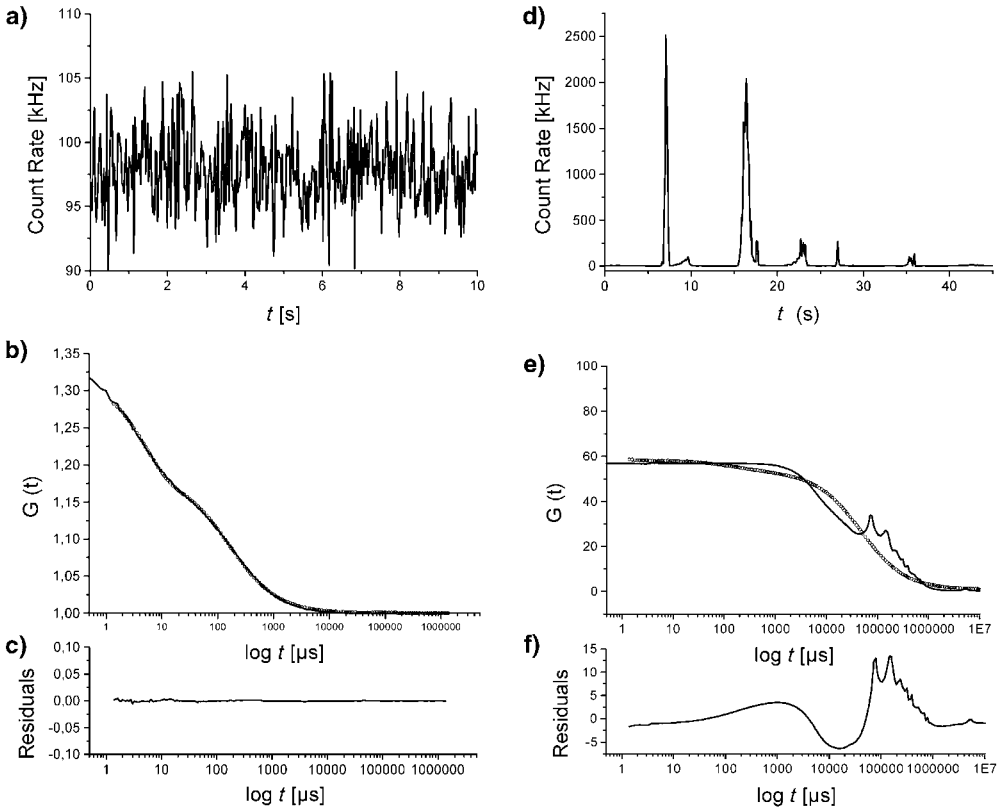

Fig. 8. *Fluorescence-correlation spectroscopy* (FCS). Testing for aggregation of oligonucleotides by **4b** and **5b**. Diffusion of Cy5-labeled $T_{20}U$ molecules (**17**) through the confocal volume element was measured as fluorescence-intensity fluctuations. Count rate *vs.* time graphs are shown in *a*) (buffer control) and *d*) (250 µM **4b**), and the corresponding autocorrelation curves (— observed; ○ calculated) are shown in *b*) (buffer control) and *e*) (250 µM **4b**). The difference between observed and calculated data points is presented as residuals in *c*) and *f*). Upon addition of **5b** up to 10 mM (not shown), the count rate *vs.* time graph shown in *a*) did not change significantly. The constant diffusion times rule out aggregation phenomena.

benzimidazoles and specific RNA ligands, and to decipher the exact cause of the artefacts described above.

Experimental Part

General. All reagents were of the highest grade commercially available. Chemicals for polyacrylamide gel electrophoresis (PAGE) were purchased from *Roth* (Karlsruhe, Germany). *NAP-10* Columns, blue dextran 2000, and the *N*-hydroxysuccinimide active ester of Cy5 (PA15101) were purchased from *Amersham Biosciences* (Uppsala, Sweden). Amino linker was obtained from *Glen Research* (Sterling, VA, USA), recombinant ribonuclease inhibitor *RNasin* ® (N2511) was from *Promega*, RNase A from *Sigma-Aldrich*, and RNase T1 from *MBI Fermentas*. TLC: glass plates precoated with silica gel *F* 254/366 (0.25 mm, *Macherey-Nagel*). M.p.: *Kofler* hot-plate microscope, uncorrected. FT-IR: *Perkin-Elmer 1600*; ν in cm^{-1}. ^{1}H-NMR: *Bruker AM-250* or *AMX-400*; chemical shifts (δ) in ppm relative to Me_4Si (0.00 ppm) or (D_5)DMSO (2.50 ppm) as internal standards, *J* in Hz. ESI-MS: *Fisons VG Platform II*. Elemental analysis: *Heraeus HCN-Rapid*.

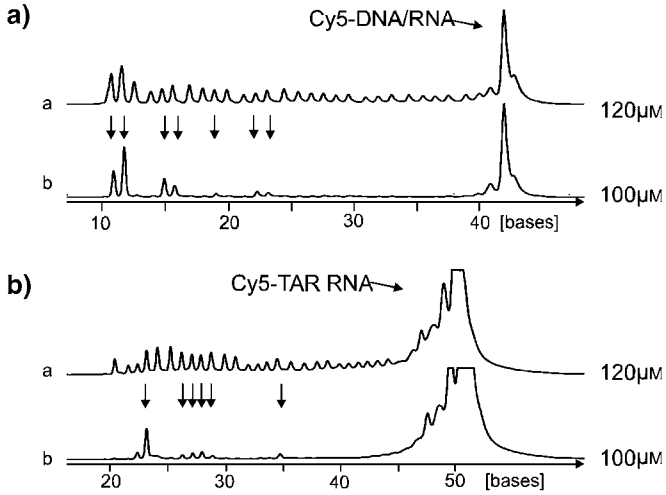

Fig. 9. *Concentration-dependent cleavage pattern induced by* **4b**. *a*) Substrate **7**. All reactions shown were performed at 120 μM (*lane a*) and 100 μM (*lane b*) catalyst concentration in 50 mM Tris-HCl, 0.01% SDS buffer (pH 6.0) under standard RNA-cleavage-assay conditions. *b*) Analogous experiments with TAR-RNA **13**. RNA fragmentation was analyzed as described in *Exper. Part*. Cleavage sites indicated by arrows are given in bold letters. **7**: Cy5-T_{10}-**CU**AG**CC**GA**C**UG**CC**GAUCUCGCUGACUGAC; **13**: Cy5-T_{20}-GGC**C**AG**AUCU**GAGC-C**U**GGGAGCUCUCUGGCC.

*Tris[2-[(4,5-dihydro-1*H*-imidazol-2-yl)amino]ethyl]amine, Salt with 2,4,6-trinitrophenol* (**5a**). Tris(2-aminoethyl)amine (0.150 ml, 1.00 mmol) was added at r.t. to a soln. of 4,5-dihydro-1*H*-imidazole-2-sulfonic acid (**6**) [11] (496 mg, 3.30 mmol) in 5 ml MeOH and 3 ml Et_3N. The mixture was stirred overnight and then diluted with 10 ml H_2O and 4 ml aq. NaOH soln. Extraction with CH_2Cl_2 removed Et_3N. The aq. phase was concentrated *in vacuo* to 50% and acidified with 5 ml 6M HCl (with release of SO_2). Complete evaporation and drying *in vacuo* yielded a mixture of product and NaCl. Product was extracted from the solid with 3 portions of boiling EtOH. The filtered EtOH solns. were then evaporated. After dissolving the residue in a small volume of MeOH, a sat. hot soln. of 2,4,6-trinitrophenol (1.18 g, 40% H_2O content, 3.10 mmol) in MeOH was added. The yellow precipitate was isolated, suspended in acetone, isolated again, and dissolved in MeOH. Insoluble, sticky material was discarded. Three recrystallizations from MeOH/H_2O finally yielded 272 mg of pure **5a** (0.260 mmol, 26%). M.p. 247°. IR (KBr): 3288*m*, 3086*w*, 2958*w*, 2901*w*, 1674*s*, 1637*s*, 1602*s*, 1566*s*, 1430*m*, 1364*m*, 1333*s*, 1267*s*, 1162*m*, 1078*m*, 909*w*, 787*w*, 711*m*. ^{1}H-NMR ((D$_6$)DMSO, 250 MHz): 2.63 (*t*, *J* = 6.5, 3 CH_2); 3.61 (*dt*, *J* = 6.4/6.1, *t* after addition of D_2O, 3 CH_2); 3.60 (s, 6 imid. CH_2); 7.4–8.5 (br. *s*, exchangeable with D_2O, NH); 7.90 (*t*, *J* = 5.3, exchangeable with D_2O, 3 NH); 8.58 (*s*, 6 arom. H, 2,4,6-trinitrophenol). Anal. calc. for $C_{33}H_{39}N_{19}O_{21}$: C 38.19, H 3.79, N 25.64; found: C 37.99, H 3.91, N 25.48.

*Tris[2-[(4,5-dihydro-1*H*-imidazol-2-yl)amino]ethyl]amine, Hydrochloride* (**5b**). A small column was filled with anion-exchange resin (*Dowex* 1 × 8, Cl^-, 200–400 mesh) and rinsed with MeOH. Filtration of 100 mg 2,4,6-trinitrophenol salt **5a** (0.096 mmol), dissolved in a small volume of MeOH, through this column afforded a colorless soln. of hydrochloride **5b** (43 mg after drying *in vacuo*; 96%). Colorless glass. ^{1}H-NMR ((D$_6$)DMSO, 400 MHz): 2.62 (*t*, *J* = 6.0, 3 CH_2); 3.30 (*q*, *J* = 5.9, *t* after addition of D_2O, 3 CH_2); 3.60 (*s*, 6 imid. CH_2); 7.7–9.0 (br. *s*, exchangeable with D_2O, 6 NH); 8.26 (*t*, *J* = 5.5, exchangeable with D_2O, 3 NH). Anal. calc. for $C_{15}H_{33}Cl_3N_{10}$: C 39.18, H 7.23, N 30.46; found: C 38.15, H 7.38, N 27.39. Note: correct analyses could not be obtained due to the hygroscopic nature of **5b**.

5′-O-*[Bis(4-methoxyphenyl)(phenyl)methyl]-2′*-O-*[*P-*(2-cyanethoxy)*-P-*(*N,N-*diisopropylamino)phosphino]-3′*-O-*[dimethyl(*tert*-butyl)silyl]uridine.* A mixture of 5′-*O*-[bis(4-methoxyphenyl)(phenyl)methyl]-3′-*O*-[dimethyl(*tert*-butyl)silyl]uridine [23] (3.30 g, 5.00 mmol) and 4-dimethylaminopyridine (60 mg, 0.50 mmol) was coevaporated with dry THF (5 ml). The solid was dissolved in dry THF (20 ml) under Ar and freshly distilled *Hünig*'s base (3.40 ml, 16.0 mmol) was added. After the dropwise addition of 2-cyanoethoxydiisopro-

pylaminophosphine (1.41 g, 6.00 mmol), the soln. was stirred for 4 h at r.t. 150 ml 5% aq. $NaHCO_3$ soln. was added and the mixture was extracted three times with 100 ml AcOEt. The combined org. layers were dried ($MgSO_4$), the solvent was evaporated and the residue was purified by flash chromatography (FC) (CH_2Cl_2/hexane 1:1 + 5% NEt_3). After drying *in vacuo,* 3.77 g (4.30 mmol, 86%) of the title compound (as a mixture of two diastereoisomers) was obtained as a colorless foam. TLC: AcOEt/hexanes 1:1 + 3% NEt_3, $R_f = 0.43$, 0.50. IR (KBr): 3412*w*, 3199*m*, 3061*w*, 2963*s*, 2931*s*, 2857*w*, 1696*s*, 1608*m*, 1582*w*, 1560*w*, 1509*s*, 1460*s*, 1202*w*, 1178*m*, 1153*w*, 1111*w*, 1069*w*, 1036*m*, 980*m*, 899*w*, 864*w*, 834*s*, 779*m*, 726*w*, 703*w*, 671*w*, 640*w*, 583*m*. ^{1}H-NMR ((D$_6$)DMSO, 400 MHz, 2 diastereoisomers): −0.04, −0.02 (2*s*, $SiMe_2$); 0.02, 0.07 (2*s*, $SiMe_2$); 0.76, 0.77 (2*s*, 2 *t*-Bu); 1.08, 1.12 (2*d*, *J* = 6.7, 4 CH(*Me*)$_2$); 2.71 (2*t*, *J* = 5.8, 2, CH_2CN); 3.19, 3.41 (2*m*, 4 C*H*(Me)$_2$); 3.59 (2*m*, 2 $H_2C(5')$); 3.74 (2*s*, 4 MeO); 3.95 (2*m*, 2 OCH_2); 4.23 (2*m*, 2 H−C(4′)); 4.31 (2*m*, 2 H−C(3′)); 4.44 (2*m*, 2 H−C(2′)); 5.38, 5.44 (2*d*, *J* = 8.0, 2 H−C(5)); 5.87, 5.94 (2*d*, *J* = 4.0, 2 H−C(1′)); 6.90 (2*d*, *J* = 8.5, 8 arom. H); 7.20–7.38 (2*m*, 18 arom. H); 7.78, 7.84 (2*d*, *J* = 8.0 Hz, 2 H−C(6)); 11.37 (*s*, 2 H−N(3)). ^{31}P-NMR ((D$_6$)DMSO, 400 MHz): 150.6, 150.5 ratio 1:1. ESI-MS: 861.8 (calc. 861.1). Anal. calc. for $C_{46}H_{65}N_4O_9PSi$: C 62.99, H 7.47, N 6.39; found C 62.90, H 7.17, N 6.51.

Assembly of Oligonucleotides. Oligonucleotides **9**–**12**, **16**, and **17** were assembled on an *Applied Biosystems 381A DNA* synthesizer by standard phosphoramidite chemistry with 2′-silylated monomers, and with 3′-silylated reagent (see above) for **10** and **12**. Compounds **7**, **8**, **13**, and **14** were purchased from *Biospring* (Frankfurt, Germany). PAGE was used to purify all oligonucleotides except **15**. Compound **15**, containing the *enantio*-RNA sequence was synthesized from 2′-*O*-tom-protected monomers [21] with an C_6-amino linker attached to the 5′ end. Coupling conditions for the active ester of Cy5: aq. borate buffer pH 8.5 (H_2O/DMF 1:1) 25°, 1 h. The final conjugate was purified by anion-exchange HPLC.

Inactivation of RNases [14]. RNA Cleavage was performed in an RNase-free environment. Glassware was baked for 6 h at 180°. During all experimental steps, gloves were worn and, when handling the reagents, sterile techniques were used. Plasticware and tubes were treated with DEPC to ensure that they were RNase-free. Solns. were prepared by mixing molecular-biology-grade powdered reagents in DEPC-treated ultrapure H_2O.

Ultrafiltration. To remove possible RNase contamination from catalysts, an ultrafiltration step (*Microcon YM3*, *Millipore*) was carried out as discribed by the manufacturer. After ultrafiltration, the filtrate was used for RNA-cleavage experiments. The retentate was discarded.

Purification of Cy5-Labeled Oligonucleotides. The Cy5-labeled oligonucleotides were purified by denaturing PAGE (16% monomer, 7M urea) to remove prematurely terminated products. After PAGE, the bands of interest were excised; the gel fragments transferred to a nuclease-free tube and submerged with elution buffer (500 mM NH_4OAc, 0.1% SDS, 2 mM EDTA) and incubated under vigorous shaking overnight at r.t. To remove the gel fragments, '*Quantum Prep Freeze'N Squeeze*' spin columns (*BioRad*, Munich, Germany) were used. Desalting of the Cy5-labeled oligonucleotides was carried out in two steps: after *YM3* ultrafiltration, the retentate was diluted to 1 ml with DEPC-treated H_2O and loaded onto a *NAP-10* column. The pooled fractions were lyophilized to dryness, and the pellet was dissolved in DEPC-treated H_2O to give a conc. of *ca.* 0.5 μg/μl.

PAGE. Prior to electrophoresis, one volume of loading buffer (5 mg/ml blue dextran in formamide) was added to each sample, and 10 μl aliquots were loaded on the gel. The oligonucleotide fragments were separated by denaturing PAGE (16% monomer, 7M urea) on a DNA-sequencing device (*ALFexpress*, *Amersham Biosciences*). Running conditions were 1500 V and 60 mA maximum at constant 30 W, 55°, 2 s sampling interval, and 350 min running time. Electropherograms were analyzed with the AlleleLinks 1.01 software package (*Amersham Biosciences*, Uppsala, Sweden). The peak areas under the curves were added, and the percentage of degraded RNA was calculated. Multiple cleavage reactions were disregarded in this system. All data were averaged over a minimum of two experiments.

RNA-Cleavage Assay. The 10 μl assays contained the indicated catalyst concentration (0.1–10 mM) and 120–140 nM of the appropriate Cy5-labeled RNA (**7**–**15**). A 50 mM *Tris*-HCl buffer containing 0.01% SDS was used: cleavage reactions with guanidinium compounds were carried out at pH 7.0, and with benzimidazole compounds at pH 6.0. The SDS prevents nonspecific binding of the RNA to the tube walls. Incubation was performed at 37° for 16–20 h. The final conc. of ribonuclease inhibitor (*RNasin*®), if applied, was 1 unit per μl.

RNase T1 Treatment: To 0.5 pmol Cy5-labeled RNA in RNase T1 incubation buffer (10 mM *Tris*-HCl, 0.02 mM EDTA, 0.3M NaCl; pH 8.0), 1 unit RNase T1 was added. After incubation for 12 min at 37°, the reaction was stopped by adding 10 μl of ALF loading buffer; 10 μl aliquots were loaded on the gel (denaturing 16% polyacrylamide (PAA) gel, electrophoresis conditions as described above).

RNase A Treatment. In a final volume of 10 μl, 0.5 pmol Cy5-labeled RNA was mixed with 10 ng RNase A in RNase A incubation buffer (6 mM *Tris*-HCl, 14% DMSO, pH 7.6). After incubation for 5 min at 37°, the reaction was stopped by adding 10 μl of ALF loading buffer, and 10 μl aliquots were loaded on the gel.

FCS Instrument. FCS Measurements were carried out with a *ConfoCor 2* (*Carl Zeiss*, Jena, Germany) equipped with an *Axiovert 200 M* microscope containing a laser-adapted *Zeiss C-Apochromat 40 × /1.2 W* corr H_2O-immersion objective. Cover slips (24 × 60 mm, *Roth*, Karlsruhe, Germany) served as sample carriers, and, for calibration of the instrument, free Cy5 dye was used. Fluctuation measurements, which are calculated in real time to give an autocorrelation curve, and further analysis, like determination of the average number and the diffusion time of the fluorescent particles in the confocal volume, were performed with the Fluorescence Correlation Microscope ConfoCor 2 Software version 3.2 SP1.

Sample Measurements. FCS Measurements were performed under conditions comparable to those used for RNA-cleavage experiments. The RNA substrates were replaced by a mixture of a Cy5-labeled $T_{20}U$ probe **17** and an unlabeled DNA oligonucleotide **16**. A final volume of 30 µl contained 25 nM Cy5-labeled $T_{20}U$, 175 nM unlabeled DNA oligonucleotide, 500–62.5 µM **4** or 10–1.25 mM **5b** in 50 mM *Tris*-HCl, 0.01% SDS buffer (pH 6.0). The incubation step (20 h, 37°) was omitted, and all FCS measurements were performed at 24°. A He/Ne laser at 633 nm was used as the excitation source. Each sample (30 µl droplet) was measured either five times for 45 s or ten times for 10 s.

REFERENCES

[1] B. Trawick, A. T. Daniher, J. K. Bashkin, *Chem. Rev.* **1998**, *98*, 939.
[2] D. M. Perreault, L. A. Cabell, E. V. Anslyn, *Bioorg. Med. Chem.* **1997**, *5*, 1209.
[3] D. M. Perreault, E. V. Anslyn, *Angew. Chem.* **1997**, *109*, 471; *Angew. Chem., Int. Ed.* **1997**, *36*, 432.
[4] J. C. Verheijen, B. A. L. M. Deiman, E. Yeheskiely, G. A. van der Marel, J. H. van Boom, *Angew. Chem.* **2000**, *112*, 377; *Angew. Chem., Int. Ed.* **2000**, *39*, 369.
[5] R. Gross, G. Dürner, M. W. Göbel, *Liebigs Ann. Chem.* **1994**, 49.
[6] K. Kurz, M. W. Göbel, *Helv. Chim. Acta* **1996**, *79*, 1967.
[7] U. Scheffer, A. Strick, E. Kalden, M. W. Göbel, in preparation.
[8] D. Brown, B. L. Pasloske, *Meth. Enzymol.* **2001**, *341*, 648.
[9] S. Klussmann, A. Nolte, R. Bald, V. A. Erdmann, J. P. Fürste, *Nature Biotechnol*. **1996**, *14*, 1112; A. Nolte, S. Klussmann, R. Bald, V. A. Erdmann, J. P. Fürste, *Nature Biotechnol*. **1996**, *14*, 1116.
[10] S. Pitsch, *Helv. Chim. Acta* **1997**, *80*, 2286.
[11] M.-S. Muche, M. W. Göbel, *Angew. Chem.* **1996**, *108*, 2263; *Angew. Chem., Int. Ed.* **1996**, *35*, 2126.
[12] B. Dietrich, D. L. Fyles, T. M. Fyles, J.-M. Lehn, *Helv. Chim. Acta* **1979**, *62*, 2763.
[13] A. Scarso, U. Scheffer, M. W. Göbel, Q. B. Broxterman, B. Kaptein, F. Formaggio, C. Toniolo, P. Scrimin, *Proc. Natl. Acad. Sci. U.S.A.* **2002**, *99*, 5144.
[14] U. Scheffer, M. W. Göbel, in 'DNA Synthesis: Methods and Protocols', 'Methods in Molecular Biology' Series, Ed. P. Herdewijn, Humana Press, Totowa, in press.
[15] C. Schmidt, R. Welz, S. Müller, *Nucleic Acids Res.* **2000**, *28*, 886.
[16] J. Hall, D. Hüsken, U. Pieles, H. E. Moser, R. Häner, *Chem. Biol.* **1994**, *1*, 185.
[17] J. Karn, *J. Mol. Biol.* **1999**, *293*, 235.
[18] M. A. Podyminogin, V. V. Vlassow, R. Giegé, *Nucleic Acids Res.* **1993**, *21*, 5950.
[19] M. A. Zenkova, N. G. Beloglazova, V. N. Sil'nikov, V. V. Vlassov, R. Giegé, *Meth. Enzymol.* **2001**, *341*, 468.
[20] N. Q. Nguyen-Trung, O. Botta, S. Terenzi, P. Strazewski, *J. Org. Chem.* **2003**, *68*, 2038.
[21] S. Pitsch, P. A. Weiss, L. Jenny, A. Stutz, X. Wu, *Helv. Chim. Acta* **2001**, *84*, 3773.
[22] J. D. Müller, Y. Chen, E. Gratton, *Meth. Enzymol.* **2003**, *361*, 69.
[23] K. K. Ogilvie, S. L. Beaucage, A. L. Schifman, N. Y. Theriault, K. L. Sadana, *Can. J. Chem.* **1978**, *56*, 2768.

Received August 25, 2003